MESSENGER X-RAY SPECTROMETER DETECTION OF ELECTRON-INDUCED X-RAY FLUORESCENCE FROM MERCURY'S SURFACE. Richard D. Starr (richard.d.starr@nasa.gov)[1,2], Larry R. Nittler[3], Shoshana Z. Weider[3], Edgar A. Rhodes[4], David Schriver[5], Charles E. Schlemm II[4], Sean C. Solomon[3], [1]Physics Department, The Catholic University of America, Washington, DC 20064, USA; [2]Solar System Exploration Division, NASA Goddard Space Flight Center, Greenbelt, MD 20771, USA; [3]Department of Terrestrial Magnetism, Carnegie Institution of Washington, Washington, DC 20015, USA; [4]The Johns Hopkins University Applied Physics Laboratory, 11100 Johns Hopkins Road, Laurel, MD 20723, USA; [5]Institute of Geophysics and Planetary Physics, University of California, Los Angeles, CA 90095, USA.

Introduction: X-ray emission from solar system bodies has been observed for decades. The surface of planets with no atmosphere may be excited by solar X-rays, solar wind particles (primarily electrons), and ions, producing line emission and bremsstrahlung. Measurements of solar-induced X-ray fluorescence from planetary surfaces have been used to infer surface elemental abundances. The MESSENGER X-Ray Spectrometer (XRS) has reported on Mercury's surface composition derived from measurements of solar-flare-induced X-ray fluorescence [1]. X-ray emissions observed from the dark side of the planet are the result of ~1-10 keV electrons impinging on the planet's surface and may also provide geochemical information.

MESSENGER XRS: The X-Ray Spectrometer (XRS) on the MESSENGER spacecraft measures elemental abundances on the surface of Mercury by detecting fluorescent X-ray emissions induced on the planet's surface by the incident solar X-ray flux [2]. The most prominent fluorescent lines are the Kα lines from the elements Mg, Al, Si, S, Ca, Ti, and Fe (1-10 keV). The XRS began orbital observations on 23 March 2011 and has observed X-ray fluorescence from the surface of the planet during both "quiet-Sun" and flaring conditions whenever a sunlit portion of Mercury has been within the XRS field of view. XRS can detect the characteristic X-rays of Mg, Al, and Si during quiet-Sun conditions, but solar flares are required to produce measurable signals from the elements of higher atomic number such as S, Ca, Ti, and Fe.

XRS Observations: X-ray fluorescence up to the Ca fluorescent line (3.69 keV) has been detected from Mercury's surface at times when the XRS field of view included only unlit portions of the planet or during quiet-Sun illumination. Many such events have been detected and are identified as electron-induced X-ray emission produced by ~1-10 keV electrons interacting with Mercury's surface. Electrons in this energy range were detected by the XRS during the three Mercury flybys, and since the beginning of orbital operations electrons of this same energy range have been detected by XRS during almost every orbit. These electron events last from minutes to tens of minutes. Electron transport models suggest that a large percentage of these quasi-trapped electrons do not complete even a single drift orbit about Mercury before impacting the surface [3]. Knowledge of the precipitating electron distribution at the planet's surface makes it possible to infer surface composition from the measured fluorescent spectra.

One example of electron-induced fluorescence is shown in Figure 1. The three XRS gas proportional counters (GPCs) clearly display fluorescence all the way up to the Ca line at 3.69 keV, despite the very limited solar output at that time. In fact, for this event on 13 August 2011, the XRS field of view was entirely filled by a dark part of the planet.

During the three MESSENGER flybys the XRS detected fluorescence and bremsstrahlung produced by electrons impinging on the detector material [4]. Since

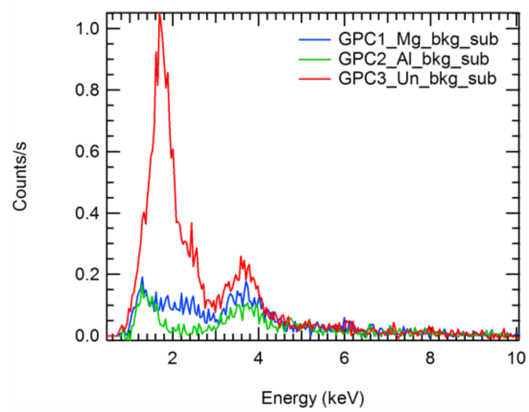

Figure 1. Example of electron-induced fluorescence from the surface of Mercury detected by XRS on 13 August 2011.

orbit insertion, similar detections are made almost every orbit near periapsis. Spectra from these events are easily identified. The two filtered detectors display fluorescence from the Mg and Al filters at 1.25 and 1.49 keV, respectively. All three GPCs display the Cu line at 8.03 keV from the XRS Be-Cu collimator as well as a bremsstrahlung continuum.

The XRS instrument response was modeled with the Monte Carlo N-Particle eXtended (MCNPX) code and verified by ground calibrations using the XRS engineering model and an electron accelerator. Results of this modeling and the good agreement with the measured spectra are described elsewhere [4]. Spectra are well modeled by kappa-function electron distributions impinging on the XRS Mg and Al filters, Be windows, and Be-Cu collimator. The inferred electron spectrum corresponding to the GPC measurements has also been described [4].

Nittler et al. [1] compared XRS results to a number of different suggested compositions and reported that the partially melted enstatite chondrite composition of Burbine et al. [5] is a reasonably good match to the observations, although not perfect. With this composition and the modeled electron flux from [4], the resulting spectrum of electron-induced X-ray fluorescence and bremsstrahlung continuum from Mercury's surface can be modeled.

Comparison of XRS Model and Measurements: More than 30 electron-induced fluorescence events have been detected by the XRS since MESSENGER entered orbit about Mercury. For most of these detections, electron and solar-induced fluorescence are combined. The electron-induced fluorescence is generally of the same magnitude as quiet-Sun fluorescence, complicating analysis. Fewer than half of these events are exclusively due to electrons. Here we focus on three such events, one on 20 May and two on 13 August 2011.

The two events from 13 August were detected about 12 hours apart and their footprints nearly overlap. The footprints of the several individual integration periods that make up these events are shown in Figure 2. Also shown in Figure 2 is the outline of the northern volcanic plains, identified by MESSENGER's Mercury Dual Imaging System [6]. The 13 August events lie just outside this region. The two events from 13 August are very similar and well described by the Burbine et al. [5] composition (Figure 3, left side). The agreement is quite good. Most other events are located in the southern hemisphere or mid-latitudes and are well described by the same model.

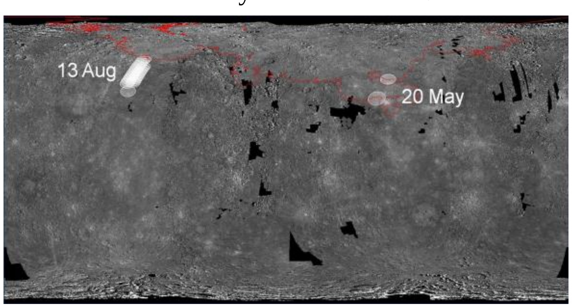

Figure 2. Footprints of electron-induced fluorescence events from 13 August 2011 and 20 May 2011. The red line is an outline of the northern volcanic plains.

One electron event that occurred over the northern volcanic plains was detected on 20 May 2011. As shown in Figure 3 (right side), this event is not well fit by the Burbine et al. [5] composition. The model (dashed line) overpredicts the flux between 1 and 2 keV. The effect of reducing the Mg composition by ~40% is shown by the solid line (model 2) in Figure 3. The lower Mg value for the northern volcanic plains has also been seen by XRS during several solar flare events [7][8].

Conclusion: The results for the electron-induced fluorescence events generally agree with XRS solar-flare measurements and show that these events may provide additional measurement opportunities for the XRS. The reliability with which the measurements are reproduced by the inferred electron spectrum [4] suggests that the electrons that interact with the XRS detector spend little time in orbit and impact the planet with minimal changes to their energy distribution.

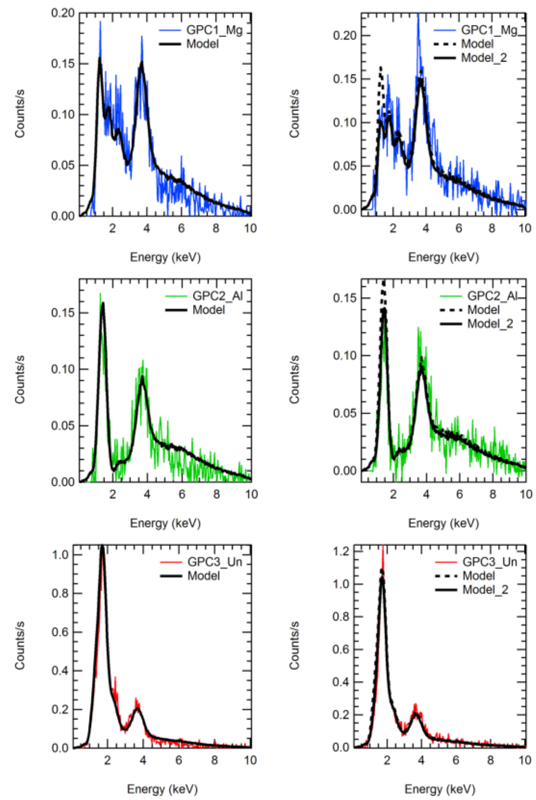

Figure 3. Model fits to electron-induced events on 13 August 2011 (left side) and 20 May 2011 (right side). The 13 August event is well described by a published compositional model [5]. The 20 May event is not well fit by this composition (dashed line) and instead requires a ~40% reduction in Mg abundance (solid line).

References: [1] L. R. Nittler et al. (2011) *Science* **333**, 1847-1849. [2] C. E. Schlemm II et al. (2007) *Space Sci. Rev.* **131**, 393-415. [3] D. Schriver et al. (2011) *Planet. Space Sci.* **59**, 2026-2036. [4] G. C. Ho et al. (2011) *Planet. Space Sci.* **59**, 2016-2025. [5] T. H. Burbine et al. (2002) *Meteorit. Planet. Sci.* **37**, 1233–1244. [6] J. W. Head et al. (2011) *Science* **333**, 1853-1856. [7] S. Z. Weider et al. (2011) *AGU* Fall Mtg., abstract P43E-04. [8] S. Z. Weider et al. (2012) *LPS*, **43**, this mtg.